Azo-hydrazone molecular switches: Synthesis and NMR conformational investigation

Kurutos, Atanas; S. Kamounah, Fadhil; M. Dobrikov, Georgi; Pittelkow, Michael; P. A. Sauer, Stephan; Hansen, Poul Erik

Published in:
Magnetic Resonance in Chemistry

DOI:
10.1002/mrc.5164

Publication date:
2021

Document Version
Peer reviewed version

Citation for published version (APA):
Kurutos, A., S. Kamounah, F., M. Dobrikov, G., Pittelkow, M., P. A. Sauer, S., & Hansen, P. E. (2021). Azo-hydrazone molecular switches: Synthesis and NMR conformational investigation. *Magnetic Resonance in Chemistry*, *59*(11), 1116-1125. https://doi.org/10.1002/mrc.5164

Kurutos Atanas (Orcid ID: 0000-0002-6847-198X)

Sauer Stephan P. A. (Orcid ID: 0000-0003-4812-0522)

Hansen Poul Erik (Orcid ID: 0000-0003-4751-9910)

Azo-hydrazone molecular switches: Synthesis and NMR conformational investigation

Atanas Kurutos, [1,*] Fadhil S. Kamounah, [2] Georgi M. Dobrikov, [1] Michael Pittelkow, [2] Stephan P. A. Sauer, [2] Poul Erik Hansen, [3]

[1] Institute of Organic Chemistry with Centre of Phytochemistry, Bulgarian Academy of Sciences, Acad. G. Bonchev str., bl. 9, 1113 Sofia, Bulgaria

[2] Department of Chemistry, University of Copenhagen, Universitetsparken 5, DK-2100 Copenhagen Ø, Denmark

[3] Department of Science and Environment, Roskilde University, DK-4000, Roskilde, Denmark

* corresponding author e-mail address: akouroutos@gmail.com (Dr Atanas Kurutos, PhD)

Abstract

A series of five intramolecularly hydrogen-bonded arylhydrazone (aryl = phenol, *p*-nitrophenol, anisole, quinoline) derived molecular switches have been synthesized and characterized by NMR and HRMS techniques. It was found that the compounds exist as different isomers in solution. An investigation of both conformational and/or configurational changes of the azo-hydrazone compounds was carried out by 1D ^{1}H- and ^{13}C- spectra, 2D NOESY, COSY, HSQC and HMBC techniques. It was found that these stimuli-responsive molecular switches exist mainly in the E form by intramolecularly hydrogen-bonded between NH and the pyridine nitrogen at equilibrium. Deprotonation of the neutral E form yields the E' deprotonated isomer. Prediction of 13C-NMR chemical shifts was achieved by DFT quantum

This article has been accepted for publication and undergone full peer review but has not been through the copyediting, typesetting, pagination and proofreading process which may lead to differences between this version and the Version of Record. Please cite this article as doi: 10.1002/mrc.5164

mechanical calculations. Anions have traditionally been difficult to calculate correctly, so calculations of the anion using different functionals, basis sets and solvent effects are also included. Deuterium isotope effects on the ^{13}C-NMR chemical shifts was employed in the assignments and furthermore utilized as indicators of intramolecular hydrogen bonding. Studies in various organic solvents including $CDCl_3$, CD_3CN and DMSO-d_6 were also performed aiming to monitor dynamic changes over several days. The effect of the hydrogen bonded solvents leads to Z-forms.

KEYWORDS: azo-dyes; molecular switches; isotope effect; ^{1}H-NMR; ^{13}C-NMR; 2D-NMR

1 | INTRODUCTION

Compounds that can take up different conformations due to a stimulus have become very important. [1] A group of these are hydrazo compounds. This type of compounds were originally investigated by Lyčka et al. [2] and later elegantly adapted as switches by the Aphrahamian group. [3] In the present paper several new hydrazo compounds are synthesized (Fig. 1) and their structures are investigated by NMR and computational calculations employing the DFT quantum mechanical approach. [4,5]

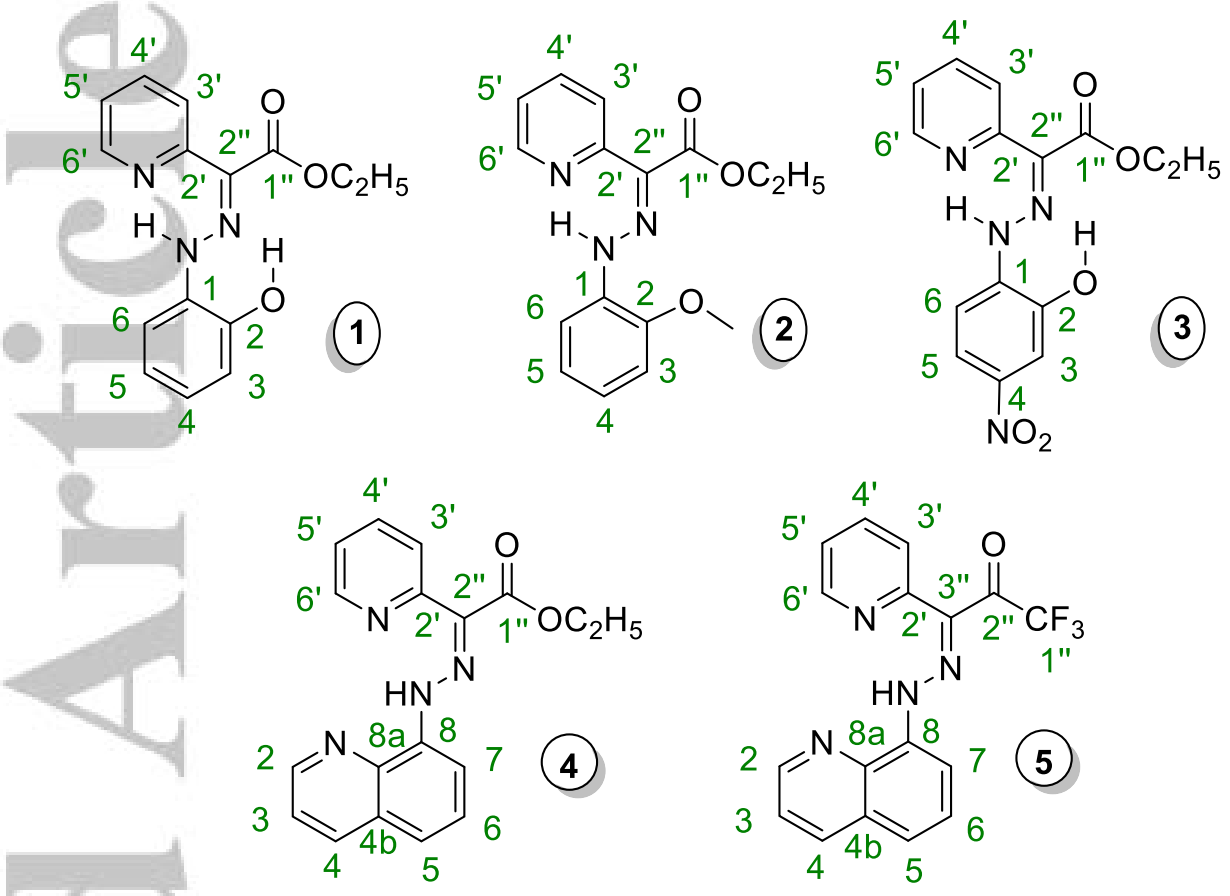

FIGURE 1 Chemical structures of the azo-dyes under investigation

Some of these molecules can exist in several different conformations (Fig. 2). Protonation-deprotonation has already been demonstrated. [3] In the present paper deprotonation is investigated to explore the structural effect of a negative charge. DFT calculations of nuclear shieldings have been shown to be a useful tool in deciding between structures or helping in determining the composition of equilibrating structures. [6] However, calculations on anions may be difficult due to large self-interactions errors. [7] Deuterium substitution is also investigated. Deuterium isotope effects on the ^{13}C chemical shifts may help in assignments as they are large over two-bonds and then fall off, but also that they are transmitted via hydrogen bonds. Furthermore, they are good indicators of intramolecular hydrogen bonds and may also be used to show the presence of tautomerism.[8,9]

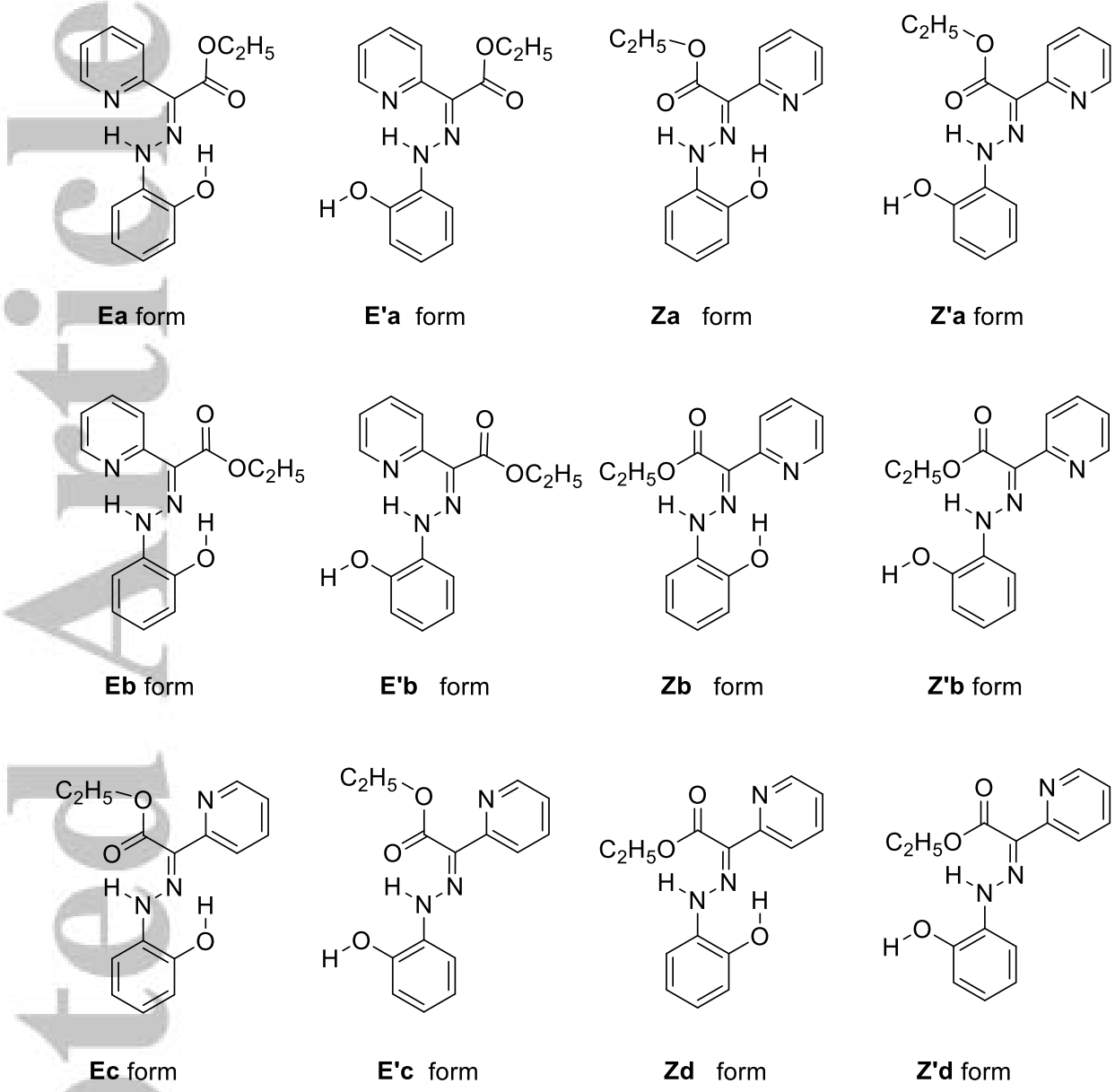

FIGURE 2 Possible conformations of compound **1**

2 | EXPERIMENTAL DETAILS

2.1 | Materials and methods

Unless otherwise stated, all starting materials and solvents required for the synthesis of the azo-dyes were purchased of purities of 99% or higher from Sigma-Aldrich, Acros Organics, Fluka, Alfa-Aesar, and used as supplied. The solvents (HPLC grade) were purchased form Sigma Aldrich and Scharlau S.L. Deuterated solvents were purchased from Sigma Aldrich and Eurisotop and used as received. Fluka silica gel/TLC-cards 60778 with fluorescence indicator

254 nm were used for monitoring the reaction progress. The spots were visualized under VILBER Ultraviolet Lamp BVL-6.LC Dual Wavelength 254/365 nm operating with power of 2×6 Watts. Purification of the dyes was done by flash column chromatography, using high-purity grade silica gel from Sigma Aldrich (pore size 60 Å, 230-400 mesh particle size). The identity of the compounds was confirmed by spectroscopic techniques including NMR and high-resolution mass spectrometry (HRMS). The detailed synthetic protocols for the preparation of the title azo-dyes along with the data related to the structural elucidation are given in the Supplementary Information.

2.2 | Deuteration experiments

Deuterium exchange was achieved by dissolving the compound in a mixture of CH_3OH and CH_3OD and evaporating off the methanol under reduced pressure in case of **1**, **2**, **4** and **5**. In case of **3** the deuteriation was achieved in DMSO-d_6 by addition of 1µl of D_2O.

2.3 | Nuclear magnetic resonance measurements

Chemical structures of the azo-dyes were evaluated using standard techniques including ^{1}H-NMR, ^{13}C-NMR, and 2-D NMR spectroscopy (COSY, HSQC, HMBC and NOESY), which were recorded on a Bruker 400 Avance III NMR spectrometer at 25 ^{o}C at 400 MHz for ^{1}H and 100.6 MHz for ^{13}C nuclei, respectively. Chemical shifts are quoted in ppm relative to the residual solvent peak as the reference standard. The chemical shifts (δ) are quoted with an accuracy of 0.01 ppm. The samples were protonated / deprotonated by the addition of trifluoroacetic acid (TFA) or tetrabutylammonium hydroxide (TBAH), respectively.

2.4 | High-resolution mass spectrometry

HRMS-MS (in CH_3CN) were recorded on a Dionex Acclaim RSLC 120 C18 2.2µm 120 Å 2.1 × 50mm column maintained at 40 °C carried out on a Bruker MicrOTOF-QII-system with ESI-source with nebulizer 1.2 bar, dry gas 8.0 L/min, dry temperature 200 °C, capillary 4500 V and plate offset -500 V.

2.5 | Calculations

The geometries were freely optimized the same way as the nuclear shieldings are calculated with the exception of the calculations with the polarization consistent basis sets, where for the geometry optimization the pc-2 basis set was employed. [10] The absence of imaginary frequencies from the calculated spectra assured that the structures correspond to a local minimum on the potential energy surface.

The shielding constants were calculated using the B3LYP functional,[4,5] basis sets 6-31g(d), the 6-311+G(2d,p), and 6-311++G(2d,p).[11,12] In addition some shielding calculations were carried out with the shielding constant version of the polarization consistent basis sets, i.e. pcSseg-2 [13,14] in combination with the pc-2 basis set for the geometry optimization. This combination was recently recommended for larger organic molecules. [15–20] In all nuclear shielding calculations the gauge including atomic orbitals (GIAO) [21–25] formalism was used. Solvent effects have been taken into account with the integral equation formalism-polarizable continuum model (IEFPCM). [26,27] Calculations were carried out using the Gaussian 16 suite of programs.[28]

3 | RESULTS AND DISCUSSION

3.1 | Structural and conformational assignment of the major forms

Having in mind that the neutral isomers, of the dyes under investigation, feature a rather similar chromophore system, the quantitation of the **E**-**Z** equilibrium in neutral state by means of UV-Vis spectroscopy is practically impossible.[29,30] Therefore, the use of the diazo NH signals from the ^{1}H NMR spectra, as suggested by Aprahamian et al., [3] remains a plausible way to quantitatively determine the **E** and **Z** isomers of a given dye present in solution.

The five compounds in the current study consist of three main components. i) A rotor, ii) axis defined along the two nitrogen atoms of the diazo-group and iii) a stator. Dyes **1**-**4** share the same ethyl 2-pyridylacetate rotor moiety, while the design of dye **5** is based on a C=OCF$_3$ group instead of the ester group. They can further be divided into those featuring a phenyl (dyes **1**-**3**) or a quinoline stator (dyes **4** and **5)**. All these compounds exist as different isomers and conformers (Fig. 2)

In the present study, three different solvents are used. Primarily CD_3CN, but also $CDCl_3$ in case of deuteriation studies and DMSO-d_6 for compounds **1** and **3**, in the latter case because of poor solubility in the other solvents.

A comparison of the assignments of the pyridine parts for all compounds **1-5** in CD_3CN shows that the chemical shifts are all rather similar (Table S1). From the NOESY spectrum of **1** in CD_3CN a cross peak from the signal at 15.15 ppm to H-6′and H-6 assigns this to NH, whereas the other high frequency resonance at 9.95 ppm shows a weak cross peak to H-3 assigning this to OH (Fig. 3). This also shows that NH is close to the pyridine ring and demonstrates hydrogen bonding to the pyridine ring.

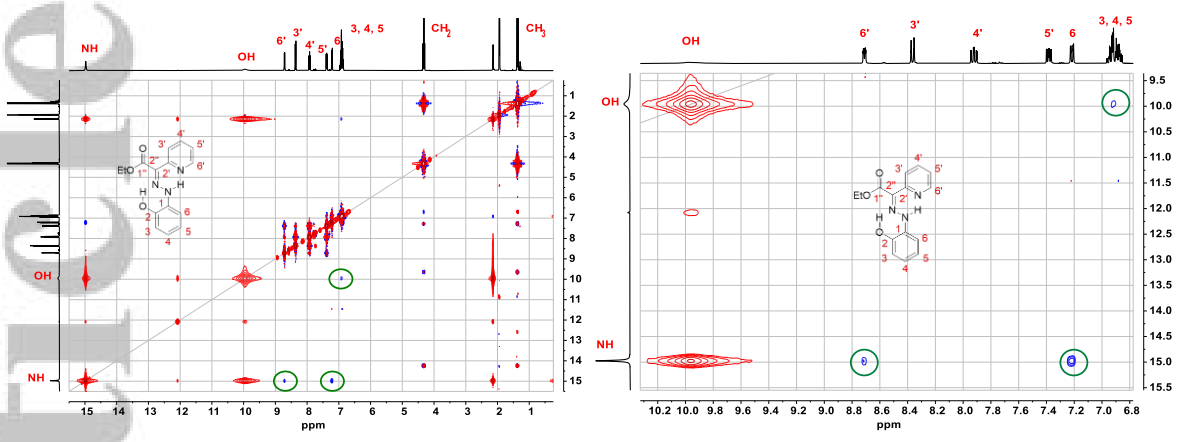

FIGURE 3 NOESY spectra of compound **1** measured in CD_3CN

The resonances of H-3, H-4 and H-5 of **1** have almost the same ^1H chemical shifts. C-4 can be identified from the HMBC spectrum due to a cross peak from H-6. However, the assignment of C-3 and C-5 in $CDCl_3$ is done as C-3 shows a large deuterium isotope effect due to deuteriation at OH (see later). The structure of the major form of **1** is E (Fig. 2).

For dye **2** a rather strong NOE cross-peak between the OCH_3 protons and H-3 shows that the OCH_3 group is primarily pointing towards H-3 (the H-3 resonance is overlapping with both H-5 and H-6 as shown in Fig. 5A, but these are too far away to give a cross peak). Even though the OCH_3 group points towards H-3, a weak cross peak is seen between the former and the NH proton, indicating that the OCH_3 group is on the same side as the NH protons as seen in E´ (See Fig. 2).

The NH chemical shift of **4** is 15.58 ppm in $CDCl_3$ showing a strong hydrogen bond to the pyridine ring. For **5** the NH chemical shift is even higher, 16.58 ppm. The structure is again the E-form.

As seen from Table 2S the chemical shifts of **1** in DMSO-d_6 are not drastically different from those in CD_3CN or $CDCl_3$. However, some differences are seen. The NOESY spectrum shows a very strong cross peak between the OH proton resonance and that of H-3 (H-3, H-5 and H-6 overlaps, but only H-3 is relevant judging from the distances. This shows that OH is pointing towards H-3. As it is not forming a hydrogen bond to N-β, it has to hydrogen bond to DMSO-d_6. In addition, a weak cross peak is seen between the water signal and H-3, H-5 or H-6. The NH proton is showing a weak cross peak to H-6´ and to either H-3, H-5 or H-6. Had it been to H-6 it would be strong as found in CD_3CN (Fig. 2). A similar trend is found for **3**. For a discussion of the preferred conformation, see calculations.

3.2 | Deuterium isotope effects on ^{13}C chemical shifts

Deuterium isotope effects on ^{13}C chemical shifts may occur if either the NH or the OH protons are exchanged with deuterium. The prerequisite for observing a ^{13}C resonance from both the H and the D species is clearly that slow exchange of the label is the case. $CDCl_3$ is usually a suitable solvent. In **1** both the NH and the OH protons are exchanged. The effects can be separated as follows: At C-1 the effect is due to deuteriation at NH judged from the magnitude (0.13 ppm).[31,32] This is also confirmed by a comparison with the results of dyes **2** (0.14 ppm), and in analogy for C-8 of the two quinoline derivatives **4** and **5** (0.13 ppm and 0.14 ppm respectively). For compound **1**, the large effect at C-2 is due to deuteriation of the OH proton (Fig. 4).

The magnitude shows that the OH group takes part in hydrogen bonding.[33] The deuterium isotope effect caused by deuteration at the NH proton is not only seen at C-1 but also at carbons in the pyridine ring due to the isotope effects being transmitted via the hydrogen bond. Transmission via the OH(D)…N hydrogen bond is also seen at C-2". C-2" is too far away for this to be a transmission via the covalent bonds. Therefore, the existence of the **E** conformation was confirmed (Fig. 2).

The isotope effects of **3** dissolved in DMSO-d_6 were obtained by adding a small amount of D_2O. [34] Due to this procedure only isotope effects due to deuteriation at the NH group is seen. An interesting observation of this deuteriation experiment is a deuterium isotope effect $^2\Delta H(D)$ at the HDO signal, whereas the OH resonance is broad. This means that the DMSO molecules are binding to water, and that the OH group is taking part in fast exchange.

For compounds **2**, **4** and **5** the isotope effects are due to deuterium exchange of the NH proton. The isotope effects are similar those seen in **1** and **3** caused by deuteriation of the NH proton.

The minor form of **2** (Z-form) (Fig. 2) shows the following isotope effects in $CDCl_3$. C=O, 0.03 ppm; C-2, 0.04 ppm; C-1, 0.12 ppm. The latter effect demonstrates that the hydrogen bond is slightly weaker (smaller two-bond isotope effect) than for the major form. The effect at C=O shows an isotope effect transmitted via the hydrogen bond.

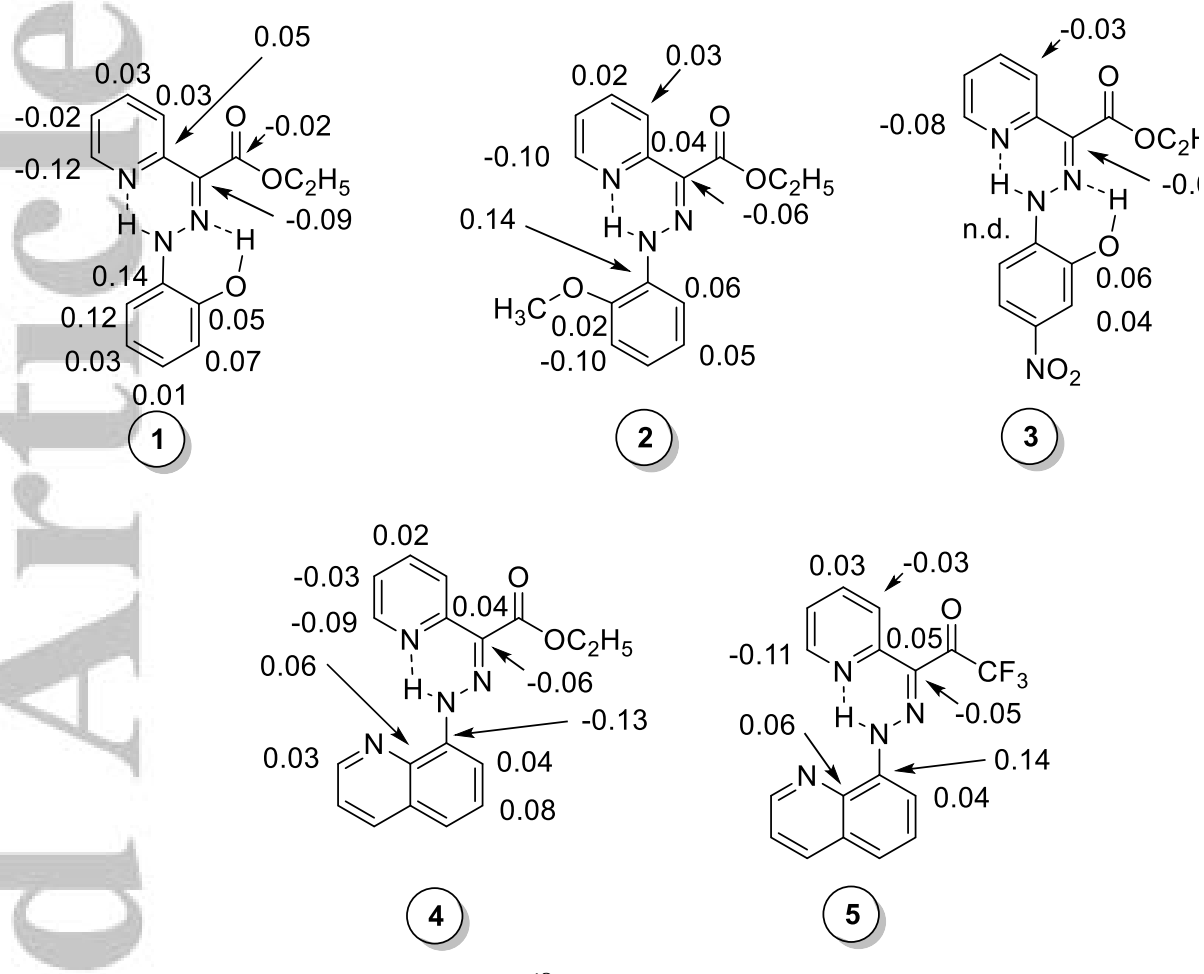

FIGURE 4 Deuterium isotope effects on ^{13}C chemical shifts of **1**, **2, 4** and **5** (in $CDCl_3$), **3** (in DMSO-d_6)

3.3 | Titrations

3.3.1 | Base addition

The titration of **1** was done in both CD_3CN and in DMSO-d_6 by adding tetrabutylammonium hydroxide (40% in water). The ^1H spectrum in CD_3CN shows no resonances due to the NH or the OH proton either due to deuteriation or to exchange (Fig. S1). The deuterium originates from the solvent as exchange of deuterium in CD_3CN occurs in the strongly basic medium. The titration results in three different species, one major and two minors. One of these develop slowly and the two minor species seem to reach an equilibrium after seven days. The latter one shows broad resonances. The ^{13}C chemical shift differences between the two minor ones are small (see TableS3). The ^{13}C NMR chemical shifts of the major charged species of **1** are summarized in Table S2. For the major form, C-2 is changing very distinctly ~12 ppm upon titration and C-5 titrates markedly, ~6 ppm compared to the neutral form. Both changes show that the OH proton is titrated.

3.3.2 | Acid addition

The NH resonance of the protonated form of **1** is observed at 13.26 ppm in CD_3CN. This signal is assigned to NH due to a cross peak to C-1 in the HMBC spectrum (Fig. S2). Furthermore, cross peaks are seen from NH to H-6 and to CH_2 in the NOESY spectrum. The OH and the NH^+ resonances are observed as an overly broad band around 8.5 ppm. The structure of **1+** is as seen a Z′ in Scheme 3.

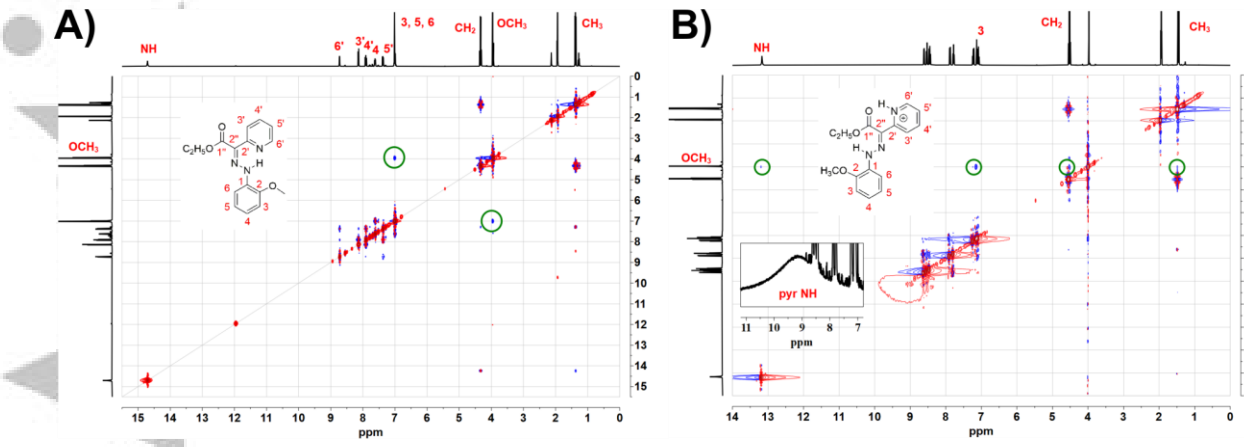

FIGURE 5 NOESY spectra of the azo-dye **2** (panel A) and the TFA-protonated azo-dye **2**

The NH resonance of the protonated form of **2** is seen at 13.17 ppm. The pyridine NH^+ is seen as an overly broad resonance at 9.5 ppm. In the NOESY spectrum a weak cross-peak is seen between the OCH_3 and H-3 and very weak ones between NH and OCH_3, CH_2 and CH_3 as shown in Fig. 5B.

3.3.3 | Minor isomer forms

The assignment of the minor forms is somewhat hampered by the low abundance. For **1** in CD_3CN no minor form can be seen in the ^{13}C spectrum. However, in DMSO-d_6, the minor form can clearly be observed. For **2** a minor form can be observed in CD_3CN, whereas **3** is recorded in DMSO-d_6. For **5** a complete assignment could also be made. The assignments are given in Table S3.

3.4 | Calculation of nuclear magnetic resonance chemical shifts

3.4.1 | Major isomer forms

Calculations of the neutral forms have been done using the B3LYP functional and 6-31G(d) basis set. This has been chosen for the neutral molecules as it gives a slightly better fit than B3LYP/6-311+G(2d,p) used later for the anion. The quality of the calculations is evaluated by plotting the experimental ^{13}C chemical shifts vs. the calculated nuclear shielding. For **1** a decent R^2 = 0.9859 is found for calculated nuclear shieldings in vacuum vs. chemical shifts in

$CDCl_3$ (a solvent with a low dielectric constant) based on the E conformation. However, for data obtained in DMSO-d_6 the correlation is very poor even including the solvent using the IEFPCM model, R^2 = 0.9704. To obtain a good R^2 = 0.9858 a DMSO-d_6 molecule should explicitly be hydrogen bonded to the OH group (Fig. 6A).

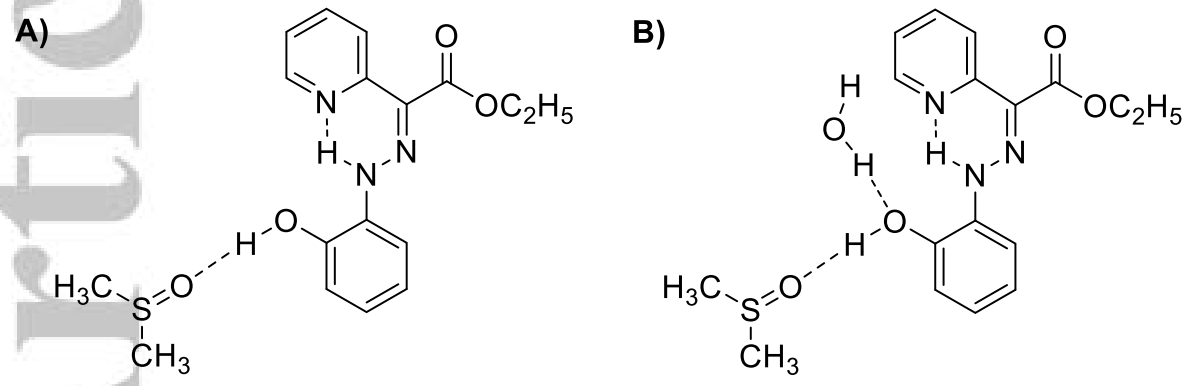

FIGURE 6 A) **1** with DMSO hydrogen bonded B) with DMSO and water hydrogen bonded

However, in that case the form is E′, as the E-form gives a R^2 = 0.9404. To get an even better correlation for the E′-form, a water molecule should be included as shown in Fig. 6b, R^2 = 0.9891. For **3** a similar conclusion can be reached in DMSO-d_6. In case of **5** a good correlation is found for the major form based on the E conformation in $CDCl_3$ (Fig. 2 and Table S2). For **5** calculations of the form with the quinoline nitrogen at the opposite site show, that this isomer is twisted and being less likely. The dihedral angle C7,C8,N,NH is 20°.

For the anion an analysis of the optimal functional and basis set had to be done. The reason is that the analysis of small negative ions can be difficult due to large self-interactions errors. [7] However, in the present case the situation is probably slightly better as the negative charge is highly delocalized. In case of $\mathbf{1}^-$ the B3LYP/6-31G(d) calculation gave a very poor fit. Even using B3LYP/6-311+G(2d,p) gives a R^2 of 0.94 for the major form. B3LYP/pcSseg-2//pc-2 gives 0.9504, whereas B3LYP/6-311++G(2d,p) gives a R^2 of 0.9533. The R^2 refers to a correlation with all carbons except the aliphatic ones. An important condition according to Jensen [35] is that the HOMO orbitals should have positive energies. This is the case. Using the PCM approximation for the solvent acetonitrile leads to a R^2 of 0.9901 for B3LYP/6-311++G(2d,p). This is slightly better than using B3LYP/pcSseg-2//pc-2 for which R^2 is 0.9846. However, the best fit is obtained by having one molecule of water hydrogen bonded to the O^- (see Fig. 7b).

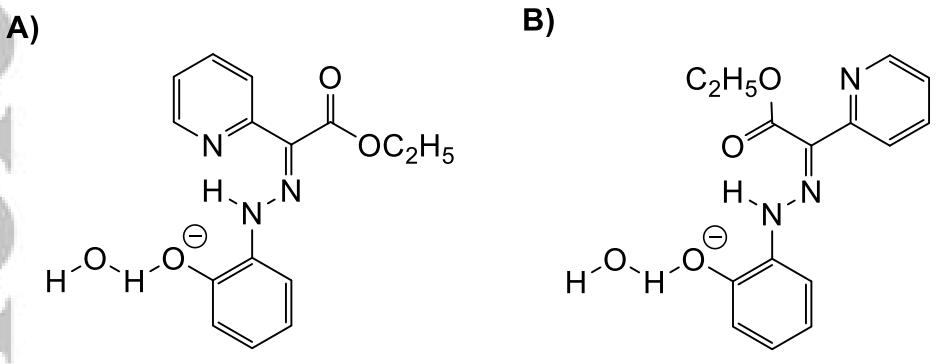

FIGURE 7 Anion of **1** hydrogen bonded to water. A) Major form. B) Minor form

In this case R^2 is 0.9974. In the latter case the pyridine is oriented with the nitrogen trans to the hydrazone N-β nitrogen as shown in Fig. This molecule has the same fit but has an energy that is 1.2 KJ lower. The counter ion, tetrabutylammonium ion, has not been included, as is too large to get close to the anion.

For **1** the minor form in DMSO is again one with a DMSO and a water molecule hydrogen bonded to the OH group as seen in Fig. 6b.

For the anion of $\mathbf{1}^-$ in acetonitrile the E′-form is preferred. For the anion itself, the IEFPCM model gives a R^2 of 0.9945 and hydrogen bonding a water to the anion only increases the R^2 to 0.950. The b-form in Fig. 2 is again preferred over the a-form by 1.2 KJ.

3.5 | Kinetics experiments

To quantitatively determine the **E** and **Z** isomers of compounds **1**, **2**, **4** and **5** in CD_3CN, $CDCl_3$ and DMSO-d_6, we recorder ^{1}H-NMR spectra of the freshly prepared solutions and over time, until E/Z equilibrium was reached. The process was monitored by the integration of the well-distinctive diazo-NH signals of the major and minor forms.

Comparing the results of Fig. 8 pairwise, we find that for **1** a fast equilibrium is established in all solvents, whereas this is only partially the case for **2**. Comparing **4** and **5**, it is in this case **5** that equilibrates very fast. For compound **4** we found that the E/Z equilibrium is established after 48-76 hours, depending on the employed solvent.

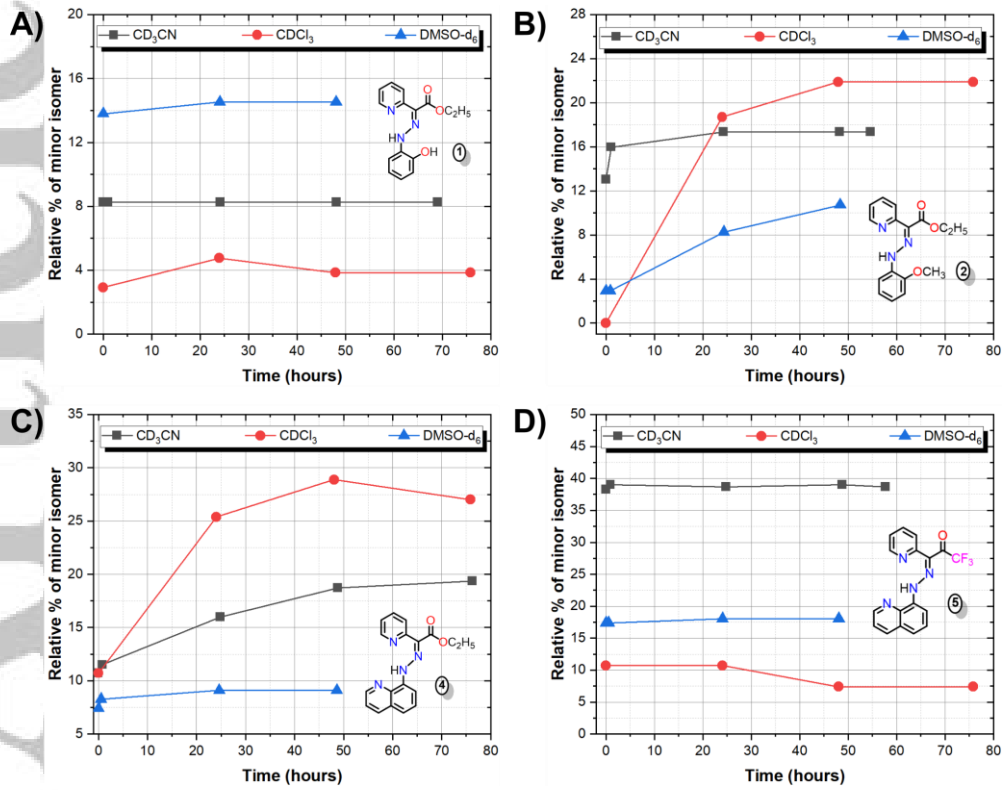

FIGURE 8 Equilibration of minor isomer over time - based on the ratio of the NH signal of the two isomers

A rather slow E→Z process was also shown earlier for the same azo-hydrazone by Deneva *et al.*, who conducted measurements in CD_3CN and Toluene-d_8. [36] The saturated isotherms of the former report point to an 82% for the E and 18% for the Z isomer after approximately 139 hours. Dye **3** is only slightly soluble so only DMSO is a suitable solvent. As can be seen from Fig. 8 a suitable solvent can be chosen for all compounds to have an almost pure major isomer from start. For **1** the fast equilibrium can be due to a contribution from the zwitterionic resonance form seen in Scheme 1a, whereas for **5** it is more likely the zwitterionic resonance form of Scheme 1b. This is supported by the finding, that the CF_3CO group enolises more easily than the ester group. [37,38]

An interesting comparison is the C=O chemical shift of the major form, the C=O group is not hydrogen bonded, whereas it is in the minor form. This should lead to a high frequency shift in the minor form compared to the major one. However, as seen from Tables S1 and S2 it is the opposite. This can be explained by the influence of the resonance form b of Scheme 1b. Furthermore, a comparison of the C=O chemical shifts in $CDCl_3$ and in DMSO-d_6 (Table S2) shows for **4** and **5** the chemical shift is the lowest in DMSO, the solvent with the highest dielectric constant. This supports the zwitterionic resonance forms.

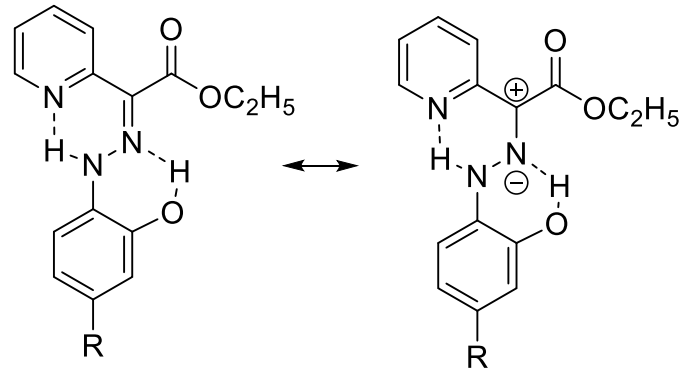

SCHEME 1a Resonance forms of the azo-dye **1**

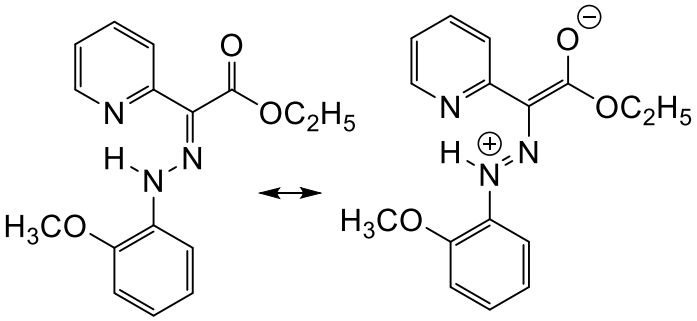

SCHEME 1b Resonance forms of dyes, **2** and after the same principle **4** and **5**

The back-conversion form minor to major needs to be fast too to arrive at an equilibrium constant of ~0.1. The OH group in position 2 seems to be important. This can be ascribed to the influence of the resonance expressed in form B (Scheme 1), which is stabilized by delocalization of the positive charge into the pyridine ring and by the intramolecular hydrogen bond. The latter is not present in **2** or in the non-substituted compounds, **4** and **5**. This could be further supported by the finding of a larger equilibrium amount of the minor form in DMSO (with a higher dielectric constant), which will favor the B resonance form.

Based on the assignment of the major and minor forms of the studied compounds it was possible to estimate the equilibrium E/Z ratio employing the same methodology as Aprahamian.[3] The ratios (major : minor isomer) and the corresponding chemical shifts of the diazo NH protons are summarized in Table 1 and Table 2.

Compound **1** reaches a spontaneous equilibrium in all studied solvents ($CDCl_3$, CD_3CN and DMSO-d_6). The same is true for the quinoline-derived dye **5** containing a CF_3 group on the rotor part. Landge *et al.* suggest a set of tautomeric equilibria involving transfer of the NH proton to the pyridine nitrogen in order to explain the height of the interconversion barrier

between the E- and the Z-form. [39] In the case of **1** a hydroxyl group in 2-position leads to a faster formation of the minor Z isomer (Fig. 6). The same was found for compound **5**, but it does not contain an OH group. This is likely due to the hydrogen bond formation and to promotion of the B resonance form of Scheme 1, as the OH proton is not acidic enough to protonate the pyridine, as is happening when adding trifluoroacetic acid. The nitro group in the 4-position of dye **3** could eventually promote either transfer of the NH proton or lead to a stronger intramolecular hydrogen bond involving the NH proton.

TABLE 1 Equilibrium mixtures of the isomers of compounds **1**-**3** determined by ^{1}H NMR

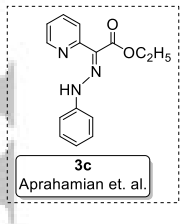

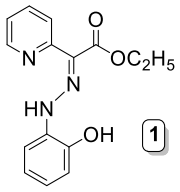

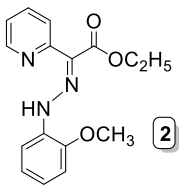

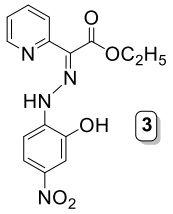

Solvent	**ratio (major : minor isomer)**		
$CDCl_3$	97 : 3	100 : 0	96 : 4
CD_3CN	92 : 8	87 : 13	Insoluble
DMSO-d_6	86 : 14	97 : 3	84 : 16
Solvent	**NH chemical shift (major : minor isomer)**		
$CDCl_3$	15.25 / 12.61	14.82 / 12.48	15.45 / 12.65
CD_3CN	14.98 / 12.08	14.71 / 11.96	Insoluble
DMSO-d_6	14.44 / 11.84	14.68 / 11.83	14.66 / 11.71

TABLE 2 Equilibrium mixtures of the isomers of compounds **4** and **5** determined by ^{1}H NMR

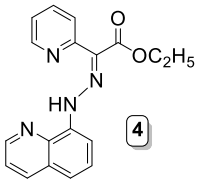

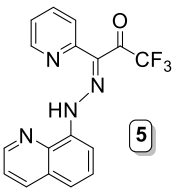

solvent	**ratio (major : minor isomer)**	
$CDCl_3$	89 : 11	89 : 11
CD_3CN	88 : 12	62 : 38
DMSO-d_6	93 :7	83 :17
solvent	**NH chemical shift (major : minor isomer)**	
$CDCl_3$	15.58 / 13.51	16.59 / 14.89
CD_3CN	15.38 / 12.95	16.54 / 14.83
DMSO-d_6	15.27 / 12.77	16.44 / 14.77

A protonation-deprotonation cycle has been demonstrated by Aprahamian et al. [3] as shown in Scheme 3. The availability of OH group in **1** gives the additional opportunity when the stimuli are applied in reverse order, namely base->acid. In this case the neutral **E**/**Z** mixture switches to **E'**/**Z'** anion mixture analogous rotation and finally the molecular switch returns to the initial state upon addition of TFA. The overall process is outlined in Scheme 3 for dye **1** as a paradigm.

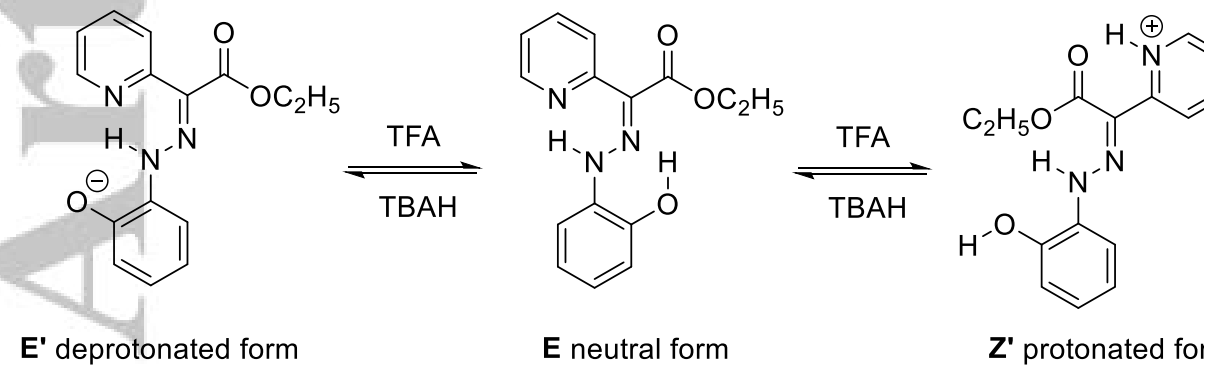

SCHEME 3 Proposed Acid/Base-catalyzed isomerization process of compound **1**. Titrations were carried out using TFA (trifluoroacetic acid), while TBAH (tetrabutylammonium hydroxide)

The illustration shows that the addition of acid to the **E'** deprotonated form leads initially to the formation of the **E** neutral form and finally to the **Z'** protonated form. In turn, the initial state can be restored by the addition of a base (TBAH used in our case). In this way a rotary switch is designed that responds by different rotation depending on the sequence of acid/base input. The exact same principle should apply to compound **3** having a nitro group on the stator.

4 | CONCLUSIONS

In this study, a series of intramolecularly hydrogen-bonded arylhydrazone (aryl = phenol, *p*-nitrophenol, anisole, quinoline) derived molecular switches were successfully synthesized and characterized by NMR and HRMS techniques. It was found that the compounds exist as different isomers in solution. For all five compounds the major isomer are on the E-form in CD_3CN and $CDCl_3$ (Fig. 3) as was also found for the non-substituted compound investigated by Aprahamian et al. [3]. For **4** and **5** the quinoline nitrogen is weakly bonded to the NH proton. This is also confirmed by X-ray studies of **4**. [40] In case of the hydrogen bonding solvent, DMSO-d_6, the major conformation is now **E´** but in that case hydrogen bonded to DMSO-d_6

(Fig. 6) and possibly also to water. The minor conformation of **2** in CD_3CN is **Z´** and so is that of **1** in DMSO-d_6, but in that case hydrogen bonded to DMSO-d_6 (Fig. 6). For the calculation of the NMR parameters of the anion of **1**, a series of test calculations led to B3LYP/6-311++G(2d,p) as the best. The preferred structure is one with a water molecule hydrogen bonded to the anion (Fig. 7). It is clear that all compounds in time equilibrate to contain varying amounts of the major and the minor form.

ACKNOWLEDGEMENTS

The authors wish to thank Annette Christensen and Britt Willer Clemmensen for their expert help in recording of the NMR spectra. The authors also wish to thank Professor L. Antonov for suggesting this research and his initial contributions. The financial support by the Bulgarian National Science Fund (BNSF) under grant DN09/10 "MolRobot" for the travelling expenses of Dr. Atanas Kurutos to Roskilde, Denmark as a postdoctoral fellow is also gratefully acknowledged.

REFERENCES

[1] S. Erbas-Cakmak, D. A. Leigh, C. T. McTernan, A. L. Nussbaumer, *Chem. Rev.* **2015**, *115*, 10081.
[2] A. Lyčka, D. Šnobl, V. Macháček, M. Večeřa, *Org. Magn. Reson.* **1981**, *15*, 390.
[3] S. M. Landge, I. Aprahamian, *J. Am. Chem. Soc.* **2009**, *131*, 18269.
[4] A. D. Becke, *J. Chem. Phys.* **1993**, *98*, 5648.
[5] C. Lee, W. Yang, R. G. Parr, *Phys. Rev. B* **1988**, *37*, 785.
[6] B. A. Saeed, R. S. Elias, F. S. Kamounah, P. E. Hansen, *Magn. Reson. Chem.* **2018**, *56*, 172.
[7] F. Nattino, C. Dupont, N. Marzari, O. Andreussi, *J. Chem. Theory Comput.* **2019**, *15*, 6313.
[8] S. Abood Hameed, S. K. Alrouby, R. Hilal, *J. Mol. Model.* **2013**, *19*, 559.
[9] L. Antonov, *Tautomerism: Concepts and Applications in Science and Technology*, John Wiley & Sons, **2016**.
[10] F. Jensen, *J. Chem. Phys.* **2001**, *115*, 9113.
[11] M. J. Frisch, J. A. Pople, J. S. Binkley, *J. Chem. Phys.* **1984**, *80*, 3265.
[12] R. Krishnan, J. S. Binkley, R. Seeger, J. A. Pople, *J. Chem. Phys.* **1980**, *72*, 650.
[13] F. Jensen, *J. Chem. Theory Comput.* **2008**, *4*, 719.
[14] F. Jensen, *J. Chem. Theory Comput.* **2015**, *11*, 132.
[15] V. A. Semenov, L. B. Krivdin, *Magn. Reson. Chem.* **2020**, *58*, 56.
[16] V. A. Semenov, D. O. Samultsev, L. B. Krivdin, *Magn. Reson. Chem.* **2020**, *58*, 532.
[17] V. A. Semenov, D. O. Samultsev, L. B. Krivdin, *Int. J. Quantum Chem.* **2020**, *120*, e26348.
[18] V. A. Semenov, L. B. Krivdin, *Magn. Reson. Chem.* **2021**, *59*, 108.
[19] D. Szunyogh, R. M. L. McFadden, V. L. Karner, A. Chatzichristos, T. D. Goodacre, M. H. Dehn, L. Formenti, D. Fujimoto, A. Gottberg, E. Kallenberg, I. Kálomista, R. F. Kiefl, F. H. Larsen, J. Lassen, C. D. P. Levy, R. Li, W. A. MacFarlane, I. McKenzie, G. D.

Morris, S. Pallada, M. R. Pearson, S. P. A. Sauer, P. Schaffer, P. W. Thulstrup, L. Hemmingsen, M. Stachura, *Dalton Trans.* **2018**, *47*, 14431.
[20] E. G. Lacerda, F. S. Kamounah, K. Coutinho, S. P. A. Sauer, P. E. Hansen, O. Hammerich, *ChemPhysChem* **2019**, *20*, 78.
[21] F. London, *J. Phys. Radium* **1937**, *8*, 397.
[22] R. McWeeny, *Phys. Rev.* **1962**, *126*, 1028.
[23] R. Ditchfield, *Mol. Phys.* **1974**, *27*, 789.
[24] K. Wolinski, J. F. Hinton, P. Pulay, *J. Am. Chem. Soc.* **1990**, *112*, 8251.
[25] J. R. Cheeseman, G. W. Trucks, T. A. Keith, M. J. Frisch, *J. Chem. Phys.* **1996**, *104*, 5497.
[26] S. Miertuš, E. Scrocco, J. Tomasi, *Chem. Phys.* **1981**, *55*, 117.
[27] S. Miertuš, J. Tomasi, *Chem. Phys.* **1982**, *65*, 239.
[28] *Gaussian 16, Revision C.01, Frisch, M. J.; Trucks, G. W.; Schlegel, H. B.; Scuseria, G. E.; Robb, M. A.; Cheeseman, J. R.; Scalmani, G.; Barone, V.; Petersson, G. A.; Nakatsuji, H.; Li, X.; Caricato, M.; Marenich, A. V.; Bloino, J.; Janesko, B. G.; Gomperts, R.; Mennucci, B.; Hratchian, H. P.; Ortiz, J. V.; Izmaylov, A. F.; Sonnenberg, J. L.; Williams-Young, D.; Ding, F.; Lipparini, F.; Egidi, F.; Goings, J.; Peng, B.; Petrone, A.; Henderson, T.; Ranasinghe, D.; Zakrzewski, V. G.; Gao, J.; Rega, N.; Zheng, G.; Liang, W.; Hada, M.; Ehara, M.; Toyota, K.; Fukuda, R.; Hasegawa, J.; Ishida, M.; Nakajima, T.; Honda, Y.; Kitao, O.; Nakai, H.; Vreven, T.; Throssell, K.; Montgomery, J. A., Jr.; Peralta, J. E.; Ogliaro, F.; Bearpark, M. J.; Heyd, J. J.; Brothers, E. N.; Kudin, K. N.; Staroverov, V. N.; Keith, T. A.; Kobayashi, R.; Normand, J.; Raghavachari, K.; Rendell, A. P.; Burant, J. C.; Iyengar, S. S.; Tomasi, J.; Cossi, M.; Millam, J. M.; Klene, M.; Adamo, C.; Cammi, R.; Ochterski, J. W.; Martin, R. L.; Morokuma, K.; Farkas, O.; Foresman, J. B.; Fox, D. J. Gaussian, Inc., Wallingford CT, 2016*, **n.d.**
[29] S. Hristova, F. S. Kamounah, N. Molla, P. E. Hansen, D. Nedeltcheva, L. Antonov, *Dyes Pigments* **2017**, *144*, 249.
[30] S. Hristova, F. S. Kamounah, A. Crochet, P. E. Hansen, K. M. Fromm, D. Nedeltcheva, L. Antonov, *J. Mol. Liq.* **2019**, *283*, 242.
[31] P. E. Hansen, A. Kolonicny, A. Lycka, *Magn. Reson. Chem.* **1992**, *30*, 786.
[32] P. E. Hansen, S. Bolvig, F. Duus, M. V. Petrova, R. Kawecki, R. Krajewski, L. Kozerski, *Magn. Reson. Chem.* **1995**, *33*, 621.
[33] P. E. Hansen, *Magn. Reson. Chem.* **1986**, *24*, 903.
[34] J. Reuben, *J. Am. Chem. Soc.* **1985**, *107*, 1756.
[35] F. Jensen, *J. Chem. Theory Comput.* **2010**, *6*, 2726.
[36] V. Deneva, N. G. Vassilev, S. Hristova, D. Yordanov, Y. Hayashi, S. Kawauchi, F. Fennel, T. Völzer, S. Lochbrunner, L. Antonov, *Comput. Mater. Sci.* **2020**, *177*, 109570.
[37] J. L. Burdett, M. T. Rogers, *J. Am. Chem. Soc.* **1964**, *86*, 2105.
[38] D. Wang, K. Ding, *Chem. Commun.* **2009**, 1891.
[39] S. M. Landge, E. Tkatchouk, D. Benítez, D. A. Lanfranchi, M. Elhabiri, W. A. Goddard, I. Aprahamian, *J. Am. Chem. Soc.* **2011**, *133*, 9812.
[40] X. Su, I. Aprahamian, *Org. Lett.* **2011**, *13*, 30.

SUPPORTING INFORMATION

Additional supporting information may be found online in the Supporting Information section at the end of this article.

Graphical Abstract

Current series of intra-molecularly hydrogen-bonded arylhydrazone molecular switches exists as different isomers in solution. They are found mainly in the E form by intra-molecular hydrogen bond between the NH and the pyridine nitrogen at equilibrium.

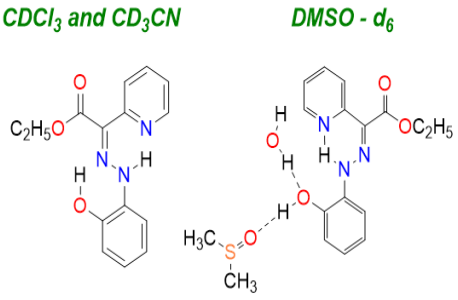

Azo-hydrazone molecular switches: Synthesis and NMR conformational investigation

Atanas Kurutos,* Fadhil S. Kamounah, Georgi M. Dobrikov, Michael Pittelkow, Stephan P. A. Sauer and Poul Erik Hansen